Relating carbon tubules

Brett I. Dunlap
Theoretical Chemistry Section, Code 6179, Naval Research Laboratory, Washington, D.C. 20375-5342
(Received 2 July 1993)

Two methods for relating different carbon tubules are described. A single graphene ribbon of infinite length but finite width can be coiled to form an infinite set of tubules, each of which has a unique pitch or helicity. This maps in a one-to-one fashion the translation/rotation operations of the group of each tubule in the set. Within the set all irreducible representations are collected into the same number of bands. Alternatively, tubules can be imagined to be pressed flat so that centers of six-member rings lie along the crease. The direction of their creases on a graphene sheet relate tubules having the same helicity but different numbers of identical rotationally symmetric subunits around their circumference. These sets help to reconcile the different expressions for band structure of tubules. These sets also help sort the various ways to join semi-infinite tubules. A perfect infinite tubule is composed entirely of hexagons. Adding one heptagon and one pentagon transforms half of the tubule into a different tubule. The two ways to group tubules suggest that the least distortion of neighboring hexagons occurs if the heptagon and pentagon are joined together or are separated to opposite sides of the tubule. In the latter case, the tubule could be imagined to be flattened so that the heptagon and pentagon are folded in half, one along each crease. This heptagon-pentagon defect best connects sets of tubules in a pairwise fashion. The paired sets of tubules have axis vectors that meet at a 30° angle on a graphene sheet. This analysis and experimental considerations suggest that the ideal bend in a tubule caused by a heptagon-pentagon pair is likely to be 30°. Because entire sets of tubules are joined in similar fashion, tailoring of tubule electronic properties can be imagined.

I. INTRODUCTION

Carbon tubules, cylinders whose walls are hexagonal graphitelike arrays of carbon atoms, are of intense experimental,[1–9] and theoretical[10–14] interest, perhaps because certain tubules promise to be the most metallic form of carbon under normal conditions[10] and because they can be made under conditions complementary to the Krätschmer-Huffman process[15] for making icosahedral C_{60}.[16] Recently single-walled tubules have been made.[17,18] In the infinite-axis-length limit all the carbon atoms in a tubule belong to six-membered carbon rings. Each ring can be equivalent by symmetry to all the rest because no one ring is topologically distinct from any other. Each six-membered ring can be viewed as a hexagon, at the vertices of which lie six carbon atoms. The hexagon must be bowed to give the curvature of the cylinder. In each hexagon there are perpendicular directions of zero and maximal curvature, thus hexagons can distort slightly upon being bent to fit the cylinderical surface.

Each hexagon on the tubule is part of three different edge-sharing spirals of hexagons.[19] Tubules can be classified by the spiral having least pitch. If this spiral is unique and if it has nonzero pitch, then the tubule is either left-handed or right-handed like a machine screw. Such chiral tubules have two symmetry-equivalent sets of atoms, members of which alternate as vertices around each hexagon. In general, these two types of atoms can have slightly different radial distance from the tubule axis. Additional mirror symmetries make the two types of atoms equivalent in the graphene layer as well as in all achiral tubules. As more and more hexagons are added to the tubule circumference, strain is relieved and the properties of the tubule surface more closely approximate those of a single sheet of graphite (a graphene layer). The strain energy of a tubule is to a good approximation inversely proportional to its radius squared.[20,21]

In reality tubules have a finite length. On occasion tubules are open at an end[3] or the ends (and outer walls) can be reacted away chemically.[22,23] Closed tubules end in caps that ideally contain exactly six pentagons,[24–27] or they evolve into more complex shapes. A single pentagon (heptagon) causes the circumference to diminish (grow) as the axis is extended beyond the defect.[3] A heptagon-pentagon pair changes one tubule into another.[28] Under the constraint of not changing a tubule into some other class of object, the heptagon-pentagon pair is the simplest topological tubule defect. By applying Euler's theorem to sp^2 carbon systems[29] the number of extra sides (relative to hexagons) in polygons larger than hexagons must equal the number of deficient sides in polygons smaller than hexagons if each atom in the tubule or graphene sheet is to remain threefold coordinated. The heptagon-pentagon pair introduces a single extra and corresponding deficient side.

This work investigates how tubules can be related to each other, both in their electronic structure and in the way in which they evolve to each other via of this simplest topological defect. Section II relates sets of perfect tubules in two ways and discusses various ways in which their electronic structure can be grouped into bands. Section III describes different heptagon-pentagon connections between tubules. Section IV argues that the optimal heptagon-pentagon connection bends the composite tubule by 30°. Section V gives some conclusions.

II. PERFECT TUBULES

The surface of the tubule can be cut in an infinite number of ways, including in a direction parallel to the tubule axis or a along line spiraling with any pitch around the axis. Every continuous nonintersecting cut from top to bottom allows the cylinder to open and become a planar graphene ribbon of infinite length. A simple ribbon results from cutting the tubule along nearest-neighbor bonds alternating between two of the generally three symmetry-distinct bonds.[28] Figure 1 shows the ribbon resulting from cutting in this manner a set of different tubules. This ribbon has an infinite height but a finite width of $L = 10$ hexagons.

This same ribbon results from unzipping an entire set of tubules that can be characterized by which corner on the right-hand side fits into which indentation on the left-hand side. The tubules are labeled (L, M) [or (M, L) if M is greater than L]. The line OM is the tubule circumference, which is perpendicular to the tubule axis. The length of this circumference is

$$OM = a\sqrt{3(L^2 + M^2 + LM)}, \tag{1}$$

where a is the length of a side of a hexagon or the nearest-neighbor carbon-carbon bond distance.

The particular ribbon depicted in Fig. 1 could have come from any tubule of the infinite set $(10, 0)$-$(10, \infty)$, and, by extending M to negative numbers, $(5, 5)$-$(9, 1)$. Extending M to even more negative values generates tubules of the opposite handedness: The set of tubules $M < -5$ becomes the set of tubules $M > -5$ upon rotation of the tubule end to end or upon reflection of the tubule through a plane parallel to the tubule axis. Except for the $(10, 10)$, $(10, 0)$, and $(5, 5)$ tubules, all tubules in the set are chiral. In fact, the tubules corresponding to $M - 10$ and $-M$ are chiral partners, i.e., enantiomers.

This ability to use a single projection to compare an entire set of tubules can be used to relate the properties of each member of the set. The group of symmetry operations of each member in this set of tubules can be mapped in a one-to-one fashion, thereby defining representations that are "close to" a given representation in each group, as "close to" was defined in an early analysis of cubic crystals.[30] Each hexagon corresponds to a unique element of the translation/rotation invariance group of each tubule. The elements of the tubule invariance group corresponds to moving a given hexagon, say the one near O in Fig. 1, to each of the remaining hexagons. The translation/rotation group is Abelian—the order of group operations is immaterial—so that each group element, corresponding to each hexagon in Fig. 1, is its own class. The complexity of the tubules groups can be further simplified. Each can have two generators that used repeatedly generate every group element, i.e., all elements of the group can be expressed a product of the first generator raised to some power and the second generator raised to some other power. Corresponding to Fig. 1, we can take the first generator to be the step of a single hexagon to the right and the second generator to be a single step up to the next row of hexagons. The irreducible representations of each group are then labeled by the phases (θ_1 and θ_2) associated with these two generators. If 2π is added to either phase, then the same representation is obtained, because all other group operations introduce a phase that is the sum of integral multiples of these two phases.

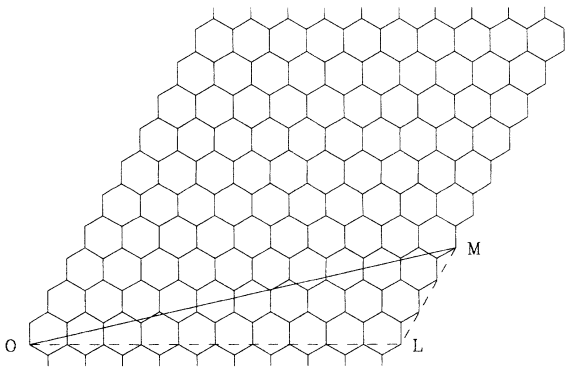

FIG. 1. A set of perfect tubules. When the left edge of the figure is mated to the right edge so that the points O and M are superposed, the (L, M) tubule is formed. In that case the line OM becomes a tubule circumference. The figure should be interpreted to extend infinitely in the skewed up-down direction.

The set of groups corresponding to Fig. 1 is bicyclic, with finite quasiperiod, ten, left-to-right and infinite period up and down. This imposes conditions on θ_1 and θ_2. The various groups in this set are distinguished by the phase-matching condition associated with the finite period, i.e., ten steps to the left is the same group element as M steps up. The requirement that the representation be single valued restricts the phases associated with the two elementary generators,

$$(e^{-i\theta_1})^L = (e^{i\theta_2})^M \tag{2}$$

or

$$L\theta_1 = M\theta_2 + n2\pi \tag{3}$$

for some integer n.

Equation (3) is the only condition on θ_1 and θ_2 independent of whether or not the tubule is translationally periodic. An ideal tubule (one having equal bond lengths and 60° bond angles) has translational periodicity, but a slight twist of the two ends can dramatically alter or even destroy the periodicity. This fact has been used to dramatically reduce the number of inequivalent atoms in a calculation that uses only translational symmetry,[34] but such a twist will not alter the phases associated with the two generators of the specific tubule group. This relationship between θ_1 and θ_2 can be visualized as straight lines on a plot of θ_2 as a function of θ_1. The slope of each line varies from -2 for $M = -L/2$ through negative infinity for $M = 0$ to approach zero as M approaches infinity. Inside the physically significant square $0 \leq \theta_1, \theta_2 \leq 2\pi$, there are portions of exactly $L + M$ such lines or bands of irreducible representations $\theta_2(\theta_1)$. Shifting this square to a physically identical square removed by $\Delta\theta_1 = \pi$, these $L + M$ bands are seen to be simple continuations of L different bands. Similarly, by shifting this square to

physically identical squares obtained by shifting θ_2 one and more increments of 2π these $L+M$ bands are seen to be simple continuations of M different bands.

These three different ways to band the irreducible representations of the tubule groups can be visualized using Fig. 1. Each of the ten vertical strips containing an infinite number of edge-sharing hexagons can be colored differently. The left and right edges can be joined into three different classes of barber poles corresponding to the three different ways of banding the irrepresentations of the tubule groups. For $0 \geq M \geq -L/2$ the $(L-M, M)$ tubules are formed. In this type of barber pole, constant colors run out of any hexagon in the $(1,-1)$ direction when L and M are measured in the $(1,0)$ and $(0,1)$ directions, respectively. For $0 \leq M \leq L$ the (L, M) tubules are formed and the constant color direction is $(0,1)$. For $L < M \leq L$ the (M, L) tubules are formed and the constant color direction is $(1,0)$. The three different edge-sharing directions out from each hexagon are symmetry equivalent for the hexagonal lattice, but differ for the tubule groups. The intraband subgroup generators are $(1,-1)$, $(1,0)$, and $(0,1)$, respectively. Plotting the band structure in these three different directions gives a more complete picture of the constraints of continuity on the electronic structure of chiral tubules.

Still other expressions of tubule band structure can be generated using nontrivial factorizations of the primitive group operations of each tubule group. Equation 2 can be written using vector notation for the group operation,

$$(0,1)^M = (L,0) = (1,0)^L \tag{4}$$

for the (L, M) tubule. From this perspective, the second group generator is the Mth root of the product of L operations of the first generator. Other nontrivial factorizations are possible. If k (direct or inverse) operations of the first generator has an integral ith root, then

$$(l,m)^i = (L,M)^j + (1,0)^k \tag{5}$$

for some set of integers j, l, k, and m. If an integral solution exists then

$$jM = im\ , \quad ilM - imL = kM. \tag{6}$$

This root (l, m) can be used as an the intraband generator. [In fact any group operation other than $N(L, M)$, $N = 0, 1, \ldots$, which are mapped onto the identity, can be used as the intraband generator.] If $i = m$ there are k bands per basis function. If $k = 1$ there are M/i bands per basis function. Derived geometrically, White *et al.*[31–33] use Eq. (6) when $j = m$, $i = M$, and $k = \pm 1$, which apparently always has an integral solution—and the corresponding electronic structure a single band per basis function—if and only if the tubule does not have rotational symmetry.

All the physical meaningful helical symmetries of the tubules been characterized and used in electronic structure calculations,[19,31–33] which, however, use different number of bands. White *et al.*[31–33] use as group generators the smallest rotation perpendicular to the tubule axis and the smallest corresponding helical operation as the intraband generator. In this approach the number of bands per basis function is N, where N is the largest common factor of L and M and is the order of the rotational group of the tubule. Klein *et al.*[19] use $(1,-1)$ as the intraband generator. Saito *et al.*[35–38] use $(1,0)$ as the intraband generator. The number of bands per basis function is different in all three methods if $L \neq N$ and $M > 0$. In this case the approach of White *et al.*[31–33] gives the minimum number and the approach of Klein *et al.*[19] gives the maximum number of bands.

The Hückel model applied to carbon assumes one basis function, the π orbital, per carbon atom, neglects basis-function overlap with neighboring atoms, and includes only a nearest-neighbor hopping matrix element V. The tubule bands can be symmetrically expressed

$$\varepsilon(\theta_1, \theta_2) = \pm V|1 + e^{i\theta_1} + e^{i\theta_2}| \tag{7}$$

about the on-site matrix element. Due to this symmetry there is no band gap (in these models) if

$$\theta_1 = -\theta_2 = n\frac{2\pi}{3} \tag{8}$$

for some representation and some integer n. Equations (3) and (8) can be combined to give the narrow-band-gap condition

$$L\frac{2\pi}{3} = M\frac{2\pi}{3} + n2\pi \tag{9}$$

for some integer n, i.e., the difference between L and M must be a multiple of three. In fact, only the (L, L) tubules are truly metallic.[10] The others are narrow- or wide-gap semiconductors depending on whether or not $L - M$ is divisible by 3.[11,35–38] The $(6,0)$ tubule[13] is narrow gap. The band gaps of wide-gap tubules, independent of chirality, are predicted to be inversely proportional to the tubule radius.[31]

The mapping of Fig. 1 groups tubules of different helical twist angles. Grouping tubules of identical helicities can be done by imagining them pressed flat like a pant leg upon ironing. Each crease of the pant leg can be aligned on a graphene sheet. When optimally creased and positioned on the graphene sheet the creases will go through the center of some hexagons as depicted in Fig. 2. In this manner the set of all tubules with the same helicity correspond to different distances between the parallel lines of the same slope. The individual members of this set of tubules can be labeled by the rotational integer N, where

$$(L, M) = N(L_\parallel, M_\parallel), \tag{10}$$

where $L_\parallel$ and $M_\parallel$ have no common integer factor. The tubules are considered flattened. Only half of their surfaces are contained within the creases of Fig. 2. Thus a $(7,1)$ dashed line in the upper part of the figure connects the creases of the $N = 2$ or $(14,2)$ tubule.

Tubules with identical helicities have axes and creases that have the same slopes on the hexagonal lattice. In fact, this slope is perpendicular to circumferential direction (L, M) used to label the tubule. For such a tubule the axial direction $(L_\perp, M_\perp)$ is a function of the circumferential direction,

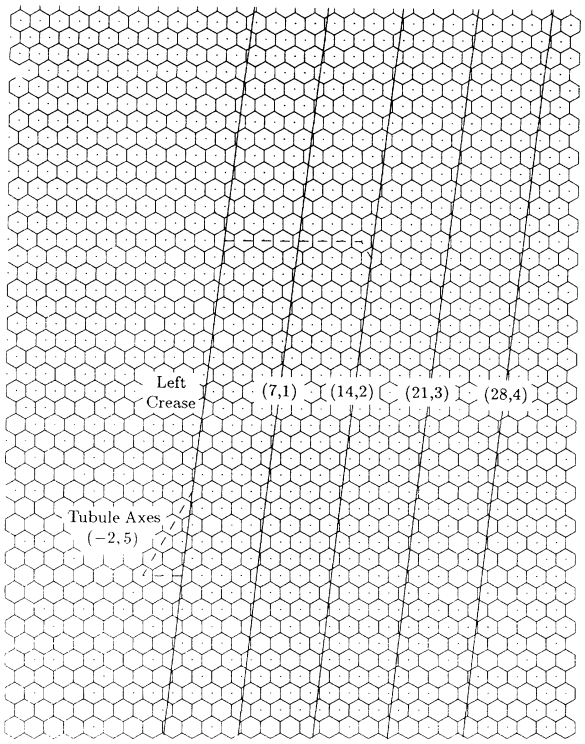

FIG. 2. The set of tubules $N(7,1)$, each of which contains N rotationally symmetric subunits. They all have a common axial direction (−2,5). Only the top half of each tubule is displayed.

$$L_\perp = -\frac{L+2M}{2L+M} M_\perp. \tag{11}$$

The use of this equation requires a fixed coordinate system, as did the specfication of intraband generator. Choosing the coordinate system of Fig. 1 gives the tubule circumference vectors as $N(8,-1)$. Equation (11) then gives the axial vector $(-2,5)$, which is indicated by the dashed triangle in the lower left of Fig. 2.

III. THE SINGLE PENTAGON-HEPTAGON PAIR DEFECT

The circumference OM of Fig. 1 cuts $L+M$ carbon-carbon nearest-neighbor bonds. Thus two tubules having the same sum $L+M$ may, in principle, be joined together coaxially while still preserving the threefold coordination of each carbon atom. A major problem with coaxially joining two tubules having the same sum $L+M$ is that the circumferences differ—most dramatically between (L,L) tubules and $(2L,0)$ tubules, which have a circumference that is larger by the factor of $2/\sqrt{3}$ or roughly 15%. This difference in circumference is easily seen by considering the quite spherical C_{60} molecule itself. Viewed down the fivefold axis and down the threefold axes the equatorial bands of hexagons can be repeated indefinitely to form (5,5) and (9,0) tubules, respectively. The circumferential mismatch for these two tubules predicted by Eq. (1) is smaller, 4%.

If a tubule is cut at increasing angles relative to the plane of its circumference, however, the circumference of the cut increases without limit. Thus any tubule can be joined to any other tubule, often in a multitude of ways. The energetically most stable junction is likely to contain the fewest defects—number of carbon rings containing other than six carbon atoms. Cutting two different tubules to have the same number of cut bonds and then seaming the two different halves together will, as a rule, introduce a large number of defects at the seam. Forcing an (L,L) tubule to join a $(2L,0)$ at a circumference of each introduces a seam of L heptagon-pentagon pairs.

It is perhaps best to study the properties of simple defects, which are likely to be more stable, than to consider directly the many ways tubules can be joined. Figure 3 shows the topology of a simple defect in a graphene sheet that preserves threefold coordination of each carbon atom and introduces a long-range tubule change. All horizontal rows of hexagons above the heptagon contain eleven hexagons and all horizontal rows below the pentagon contain ten polygons. The topological distortion incorporated into Fig. 2 makes it clear that the left and right edges of the figure can be joined, as in Fig. 1, to form a set of compound tubules, in which (L,M) and $(L+1,M)$ semi-infinite tubules are joined. For all these joints only one abutting pentagon-heptagon pair is required.

One or more hexagons can be introduced between the heptagon and pentagon of Fig. 3. If a sequence of n hexagons are joined across opposite sides to connect the heptagon and pentagon, then the number of hexagons across the top of a corresponding figure would be $11+n$. The distortion of such a figure plotted in the planar manner of Fig. 3 increases dramatically with n. Such distortion in an sp^2 carbon network means that some carbon atoms must either bend out of the plane or have have bonds that differ significantly from the ideal hexagonal bond distance, both of which exact a high penalty in energy.

A more practical way to consider the effect of increasing the distance between the hepatgon and pentagon in Fig. 3 is based on the pressed tubule representation of Fig. 2. A heptagon or a pentagon could be folded in half

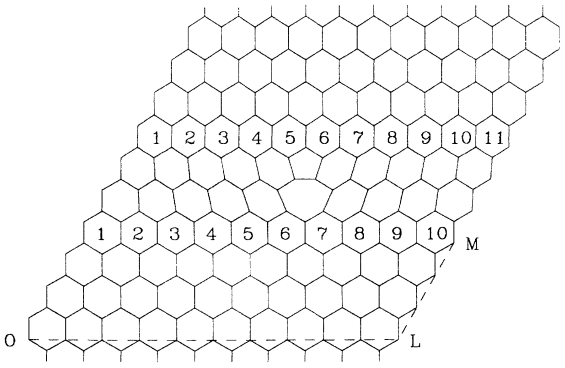

FIG. 3. Same as Fig. 1, but containing a heptagon-pentagon defect. There are eleven hexagons in each row above the pentagon and only ten in each row below the heptagon.

along either crease. For a heptagon 7/2 sides lie to either side of the crease. For a pentagon 5/2 sides lie to either side of the crease. This result is independent of the orientation of the polygons relative to the crease direction, it relies only on the fact that the crease went through the center of the polygon. The two creases running through the heptagon and through the pentagon are readily depicted on a planar suface. The heptagon bends the line at a $7/6\ \pi$ angle and the pentagon bends the line at a $5/6\ \pi$ angle. The two creases are parallel in the pure tubule region far enough from the defect. These two sets of parallel lines can be extended to meet at the pentagon and heptagon. If the creases are at the opposite sides of the tubule, then the tubule lies flat like a pressed pant leg. In that case the pentagon is at the knee, the heptagon is inside the knee, and the pant leg bends 30° at the knee.

A 30° connection between pressed tubules joins (L, L) and $(L', 0)$ tubules[28] and is drawn in Fig. 4. The two lines coming up from the bottom represent a $(12, 0)$ tubule. The first heptagon encountered shows how this tubule can be connected to the much fatter $(12, 12)$ tubule. The circumference of the seam indicated by a dashed line, which runs in a $(1, 0)$ direction, is larger than the circumference of the both tubules. The next heptagon encountered going up connects the $(12, 12)$ tubule to a $(8, 8)$ tubule. The circumference of this seam, in the $(1, 1)$ direction, is equal to the circumference of the $(8, 8)$ tubule, thus the circumference of an ideal (equal unit bond lengths) $(8, 8)$ tubule must be larger than that of an ideal $(12, 0)$ tubule. Skipping a heptagon, the $(6, 6)$ tubule meets the $(12, 0)$ tubule at the latter's circumference, thus the circumference of an ideal $(6, 6)$ tubule is less than that of an ideal $(12, 0)$ tubule. Joining the intermediately sized $(7, 7)$ tubule makes a symmetrical seam that is 15° out of the plane of the circumference of both tubules. Finally the $(3, 3)$ tubule can be connected to the $(12, 0)$ tubule, with a very large seam. Thus all (L, L) tubules can be connected to the $(12, 0)$ tubule using a single heptagon and a single pentagon. Similarly all $(L, 0)$ tubules can be connected to the $(12, 12)$ tubule. This (L, L) to $(L', 0)$ connection preserves a mirror symmetry of these achiral tubules.

If an infinite tubule is cut at some angle θ relative to the plane of the tubule circumference, then the circumference of the cut is an ellipse, ignoring any relaxation caused by the cut itself. For the unrelaxed cut, the minor axis of the ellipse is the tubule diameter. The major axis is elongated by a factor of $\sec(\theta)$. Thus the seam caused by the heptagon-pentagon pair will be most circular when the seam makes a 15° angle to the plane of both tubules. In this sense the $(12, 0)$-$(7, 7)$ connection in Fig. 4 is ideal. Equation (1) predicts the circumferential

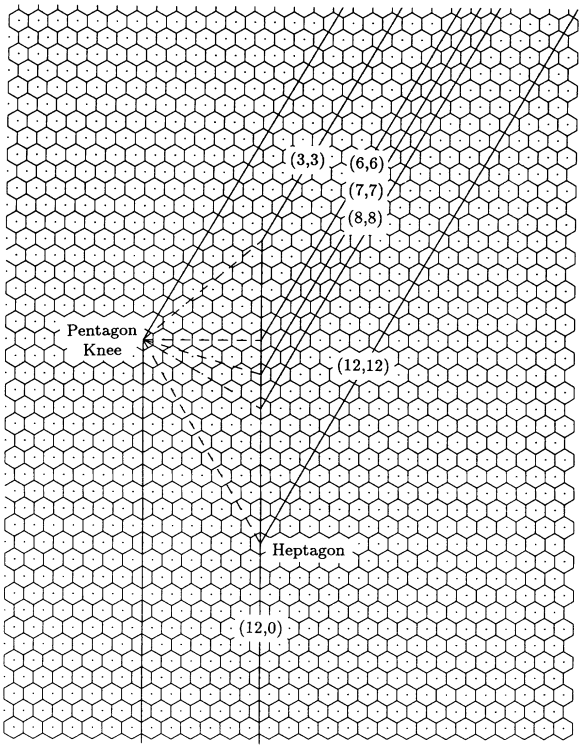

FIG. 4. Connecting the $(12, 0)$ tubule to the $(12, 12)$, $(8, 8)$, $(7, 7)$, $(6, 6)$, and $(3, 3)$ tubules with a heptagon-pentagon pair. The pentagon occurs at the knee to the left of the figure. The heptagons occur at the inside of the knee along the right edge of the pressed $(12, 0)$ tubule. The heptagon for the $(12, 12)$ connection lies lowest and the heptagon for the $(3, 3)$ lies higest in the figure. The seams between the half-tubule pairs are indicated by dotted lines.

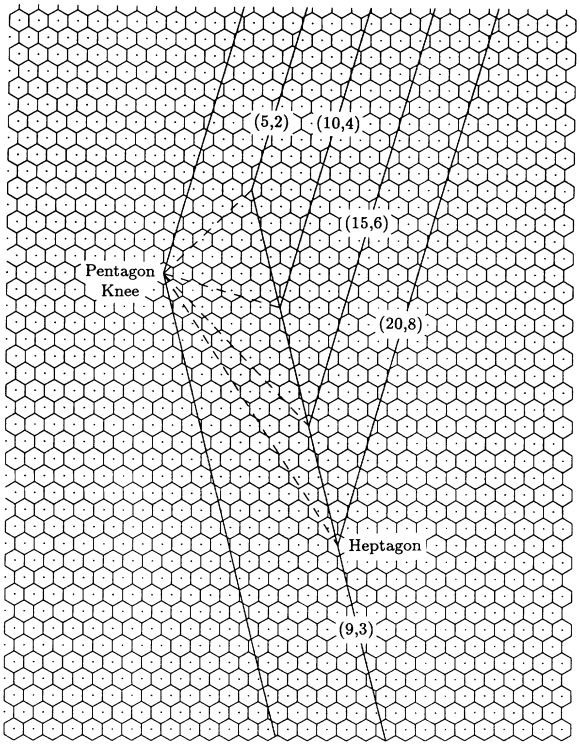

FIG. 5. Connecting the $(9, 3)$ tubule to the $(20, 8)$, $(15, 6)$, $(10, 4)$, and $(5, 2)$ tubules with a heptagon-pentagon pair. The pentagon occurs at the knee to the left of the figure. The heptagons occur at the inside of the knee along the right edge of the pressed $(9, 3)$ tubule. The heptagon for the $(20, 8)$ connection lies lowest and the heptagon for the $(5, 2)$ lies higest in the figure. The seams between the half-tubule pairs are indicated by dotted lines.

mismatch to be about 1% for this ideal connection. For the other connections, the tubule with the largest radius must flatten perpendicular to the heptagon-pentagon direction as the seam is approached.

If the tubule axes intersect at any angle, then the planes of the circumferences intersect at the same angle. Thus the tubule labels viewed as vectors intersect at the same angle. The condition that tubule (J,K) intersect (L,M) at 30° yields

$$(J,K) \propto (2L^2 - LM + M^2, L^2 - LM + M^2). \quad (12)$$

This equation does not appear to have a solution $(J,K) \propto (M,L)$ for some set of four small integers. The existence of such an L and M would imply that a tubule could be connected effectively to itself via a heptagon-pentagon pair. A set of four small integers that comes close to matching this condition is $(3,1)$ and $(5,2)$. Figure 5 shows a $3(3,1) = (9,3)$ tubule coming up from the bottom and connecting in turn to $(20,8)$, $(15,6)$, $(10,4)$, and $(5,2)$ tubules. By construction, the two sets of parallel lines are both approximately 15° from the vertical, the lines meet at exactly 30°, and the folded heptagon and pentagon have circumferences of exactly 7 and 5 ideal (hexagon) sides, respectively. Because the set of connecting tubules $N(5,2)$ is less dense in the plane, the best fit, $(9,3)$ to $(10,4)$, is less ideal than the $(12,0)$-$(7,7)$ connection in Fig. 4. Similarly, any of the $N(3,1)$ tubules can be connected via a heptagon-pentagon pair to any of the tubules above the knee of Fig. 5.

IV. DISCUSSION

The topologically gentlest transitions between tubules requires only a single heptagon and a single pentagon. If the pair of polygonal defects are near to each other in the sense of being surrounded by carbon hexagons that are locally rather flat, then there is much local distortion in the carbon lattice as shown in Fig. 1. The distortion increases as the heptagon and pentagon are pulled apart (by inserting transverse rows of hexagons). This distortion can be relieved by curvature. Thus if L is large enough, then for the entire set of tubules drawn in Figs. 1 and 2, the heptagon-pentagon pair should either abut or be moved far enough apart that there be significant curvature between them. Otherwise, the tubule joint would be expected to be relatively unstable.

The heptagon and pentagon defects individually can be thought of as being formed by adding and removing, respectively, a 60° wedge of carbon atoms from a graphene layer. These defects are negative and positive 60° disclinations, respectively, that require distortion out of the plane if the elastic constants in the plane are much larger than those out of the plane as is the case for the graphene sheet.[39–41] At a large radius from each defect the circumference is one-sixth too large and too small, respectively, when compared to the unaltered sheet. At each large radius from the defect a circumference can be drawn, which can be imagined to be constrained to the surface of a sphere of the same radius. For the pentagon the circumference is too small by one-sixth for it to be an equator, but it can still be a circle if it drops down to lattitude of $-\cos^{-1}(5/6)$. Connecting the set of circles for all large radii forms a cone that can be continued to the apex. The intersection of this cone and any plane containing its axis is a line that is bent at 67.1°. The circumference associated with a heptagon is too large to be a circle on the corresponding sphere. If whatever shape is assumed by this longer circumference on the surface of the sphere is rotated on the sphere to minimize its farthest excursions from the equator, then the equator must be crossed at least four times. Assuming the shape to be four symmetric, connected geodesics the bounding lattitudes are $\pm\cos^{-1}(6/7)$. Connecting the set of curves for all large radii a simple creased saddle point is formed that can be continued to its vertex. The crease lines bend at the vertex through angles of ±62.0°.

This analysis suggests that heptagon-pentagon defect could perhaps bend a tubule by slightly more than 60°. On the surface of a tubule, however, there is no curvature in the axial direction and maximal curvature in the circumferential direction. On its surface, the cone associated with a pentagon will distort to have a increased bend in the circumferential direction and, correspondingly, a decreased bend in the axial direction. The asymmetry could be quite large, particularly for small diameter tubules. This geometrical analysis is not inconsistent with the optimal bend angle caused by a heptagon-pentagon pair being 30°. Experimentally, the bend angle associated with both a pentagon and a heptagon on a small-diameter tubule can be measured to be close to 30° in Fig. 1 of Ref. 3.

A tubule with twelve 30° bends can be brought full circle to form a torus.[28] On the other hand, an icosahedral C_{60} can be aligned through two opposed pentagons, opened up by replacing the remaining ten pentagons with heptagons, and then closed into a C_{360} torus by a tire-shaped segment containing ten pentagons.[42] Similarly all the icosahedrically symmetric Goldberg polyhedra[43] can be inverted to form a set of related fivefold rotationally symmetric tori.[44] The C_{360} torus can be reduced by abutting pairs of heptagons to yield fivefold symmetric C_{340}.[45] In these tori each heptagon-pentagon pair can be associated with a bend of 36°. Of course, a finite section of tubule with zero or any number of heptagon-pentagon pairs can be bent and joined to form a torus. Tori found in nature, however, are likely to have optimal joints with optimal bend angles. While tori have not yet been found, open ends of tubules that curl over on themselves and continue on to form an outer wall can be considered elongated half tori.[3,46] These half tori are found to contain six heptagon-pentagon pairs. In principle, two such half tori could be joined together in a torus having twelve pairs. Perhaps the binding energy per carbon atom in the fivefold symmetric tori[42,44,45] could be increased by adding a sixth wedge equivalent to the other five and then reoptimizing the geometry. Of course, one would expect the same trend with tori that are found in fullerenes, namely, the more carbon atoms the structure contains the more stable it is.[47] This effect will add to the energy lowering obtained by inserting an additional wedge to the fivefold tori.

V. CONCLUSIONS

Carbon tubules can be related in a number of ways. Figure 1 relates the set of tubules that can be made from a bundle of ten coiled helices. Figure 2 relates tubules with the same axial direction. The relationships make transparent certain ways in which electronic states can be grouped into bands. A heptagon-pentagon pair is sufficient to connect two different tubules. Viewed as a coil of helical strands, the number of such strands changes with the number of hexagons joining the heptagon and the pentagon in a linear, acene fashion. Increasing significantly the number of strands requires curvature along the line of hexagons if the all six-membered-ring carbon-carbon bond lengths are to remain relatively constant.

Parallel creases in the two semi-infinite tubules that have been connected can be associated with the heptagon and the pentagon. The strain caused by these defects is probably least if these creases are symmetrically placed behind and in front of the knee, respectively. If this is the optimal connection between two half tubules, then 30° bends should be fairly common and the potential for modifying the electronic properties of tubules by introducing a small number of defects is great. Figure 4 shows that all the metallic tubules can be connected to the narrow-gap (12,0) tubule. Similarly, all the metallic tubules be connected to a wide-gap (14,0) tubule. The effect of the wide-gap section can be altered both by changing its diameter[31] and by changing its length. More control, still, is possible if concentric tubules with different electronic properties[38,48] could be modified in concert.

ACKNOWLEDGMENTS

I thank Sumio Iijima for Ref. 46 prior to publication and Carter White, John Mintmire, Rick Mowrey, Judith Harrison, and Daniel Robertson for useful discussions. This work was supported in by the Office of Naval Research through the Naval Research Laboratory.

[1]S. Iijima, Nature **354**, 56 (1991).
[2]S. Iijima, T. Ichihashi, and Y. Ando, Nature **356**, 776 (1992).
[3]S. Iijima, P. M. Ajayan, and T. Ichihashi, Phys. Rev. Lett. **69**, 3100 (1992).
[4]P. M. Ajayan and S. Iijima, Nature **358**, 23 (1992)
[5]T. W. Ebbesen and P. M. Ajayan, Nature **358**, 220 (1992).
[6]H. Hiura, T. W. Ebbesen, K. Tanigaki, and H. Takahashi Chem. Phys. Lett. **202**, 509 (1993).
[7]P. J. Harris, M. L. H. Green, and S. C. Tsang, J. Chem. Soc. Faraday Trans. **89**, 1189 (1993).
[8]M. José-Yacamán, M. Miki-Yoshida, L. Redón, and J. G. Santiesteban, Appl. Phys. Lett. **62**, 657 (1993).
[9]Y. Saito, T. Yoshikawa, M. Inagaki, M. Tomita, and T. Hayashi, Chem. Phys. Lett. **204**, 277 (1993).
[10]J. W. Mintmire, B. I. Dunlap, and C. T. White, Phys. Rev. Lett. **68**, 631 (1992).
[11]N. Hamada, S. Sawada, and A. Oshiyama, Phys. Rev. Lett. **68**, 1579 (1992).
[12]M. S. Dresselhaus, G. Dresselhaus, and R. Saito, Phys. Rev. B **45**, 6234 (1992).
[13]E. G. Gal'pern, I. V. Stankevich, A. L. Chistyakov, and L. A. Chernozatonskii, Pis'ma Zh. Eksp. Teor. Fiz. **55**, 469 (1992) [JETP Lett. **55**, 483 (1992)].
[14]K. Tanaka, K. Okahar, M. Okada, and T. Yamabe, Chem. Phys. Lett. **191**, 469 (1992).
[15]W. Krätschmer, L. D. Lamb, K. Fostiropoulos, and D. R. Huffman, Nature **347**, 354 (1990).
[16]H. W. Kroto, J. R. Heath, S. C. O'Brien, R. F. Curl, and R. E. Smalley, Nature **318**, 163 (1985).
[17]S. Iijima and T. Ichihashi, Nature **363**, 603 (1993).
[18]D. S. Bethune, C. H. Klang, M. S. de Vries, G. Gorman, R. Savoy, J. Vazquez, and R. Beyers, Nature **363**, 605 (1993).
[19]D. J. Klein, W. A. Seitz, and T. G. Schmalz, J. Phys. Chem. **97**, 1231 (1993).
[20]D. H. Robertson, D. W. Brenner, and J. W. Mintmire, Phys. Rev. B **45**, 12592 (1992).
[21]S. Sawada and N. Hamada, Solid State Commun. **83**, 917 (1992).
[22]S. C. Tsang, P. J. F. Harris, and M. L. Green, Nature **362**, 520 (1993).
[23]P. M. Ajayan, T. W. Ebbesen, T. Ichihashi, S. Iijima, K. Tanigaki, and H. Hiura, Nature **362**, 522 (1993).
[24]G. B. Adams, O. F. Sankey, J. B. Page, M. O'Keefe, and D. A. Drabold, Science **256**, 1792 (1992).
[25]M. Fujita, R. Saito, G. Dresselhaus, and M. S. Dresselhaus, Phys. Rev. B **45**, 13834 (1992).
[26]M. S. Dresselhaus, G. Dresselhaus, and R. Saito, Solid State Commun. **84**, 201 (1992).
[27]M. Endo and H. W. Kroto, J. Phys. Chem. **96**, 6941 (1992).
[28]B. I. Dunlap, Phys. Rev. B **46**, 1933 (1992).
[29]T. G. Schmaltz, W. A. Seitz, D. J. Klein, and G. E. Hite, J. Am. Chem. Soc. **110**, 1113 (1988).
[30]L. P. Bouckaert, R. Smoluchowski, and E. Wigner, Phys. Rev. **50**, 58 (1936).
[31]C. T. White, D. H. Robertson, and J. W. Mintmire, Phys. Rev. B **47**, 5485 (1993).
[32]J. W. Mintmire, D. H. Robertson, B. I. Dunlap, R. C. Mowrey, D. W. Brenner, and C. T. White, in *Electrical, Optical, and Magnetic Properties of Organic Solid State Materials*, edited by L. Y. Chiang, A. F. Garito, and D. J. Sandman, MRS Symposia Proceedings No. 247 (Materials Reserach Society, Pittsburgh, 1992), p. 339.
[33]C. T. White, J. W. Mintmire, R. C. Mowrey, D. W. Brenner, D. H. Robertson, J. A. Harrison, and B. I. Dunlap, in *Buckminsterfullerenes*, edited by W. E. Billips and M. A. Ciufolini (VCH, New York, 1993), p. 125.
[34]J.-Y. Yi and J. Bernholc, Phys. Rev. B **47**, 1708 (1993).
[35]R. Saito, M. Fujita, G. Dresselhaus, and M. S. Dresselhaus, in *Electrical, Optical, and Magnetic Properties of Organic Solid State Materials* (Ref. 32), p. 333.
[36]R. Saito, M. Fujita, G. Dresselhaus, and M. S. Dresselhaus, Phys. Rev. B **46**, 1804 (1992).
[37]R. Saito, M. Fujita, G. Dresselhaus, and M. S. Dresselhaus, Appl. Phys. Lett. **60**, 2204 (1992).
[38]R. Saito, G. Dresselhaus, and M. S. Dresselhaus, J. Appl.

Phys. **73**, 494 (1993).
[39]R. deWit, J. Appl. Phys. **42**, 3304 (1971).
[40]H. S. Seung and D. R. Nelson, Phys. Rev. A **38**, 1005 (1988).
[41]J. Tersoff, Phys. Rev. B **46**, 15 546 (1992).
[42]S. Itoh, S. Ihara, and J. Kitakami, Phys. Rev. B **47**, 1703 (1993).
[43]M. Goldberg, Tohoku Math. J. **43**, 104 (1937).
[44]S. Ihara, S. Itoh, and J. Kitakami, Phys. Rev. **47**, 12 908 (1993).
[45]L. A. Chernozatonskii, Phys. Lett. **170**, 37 (1992).
[46]S. Ijima, Mater. Sci. Engineering B **19**, 172 (1993).
[47]B. I. Dunlap, Phys. Rev. B **47**, 4018 (1993).
[48]J.-C. Charlier and J.-P. Michenaud, Phys. Rev. Lett. **70**, 1858 (1993).